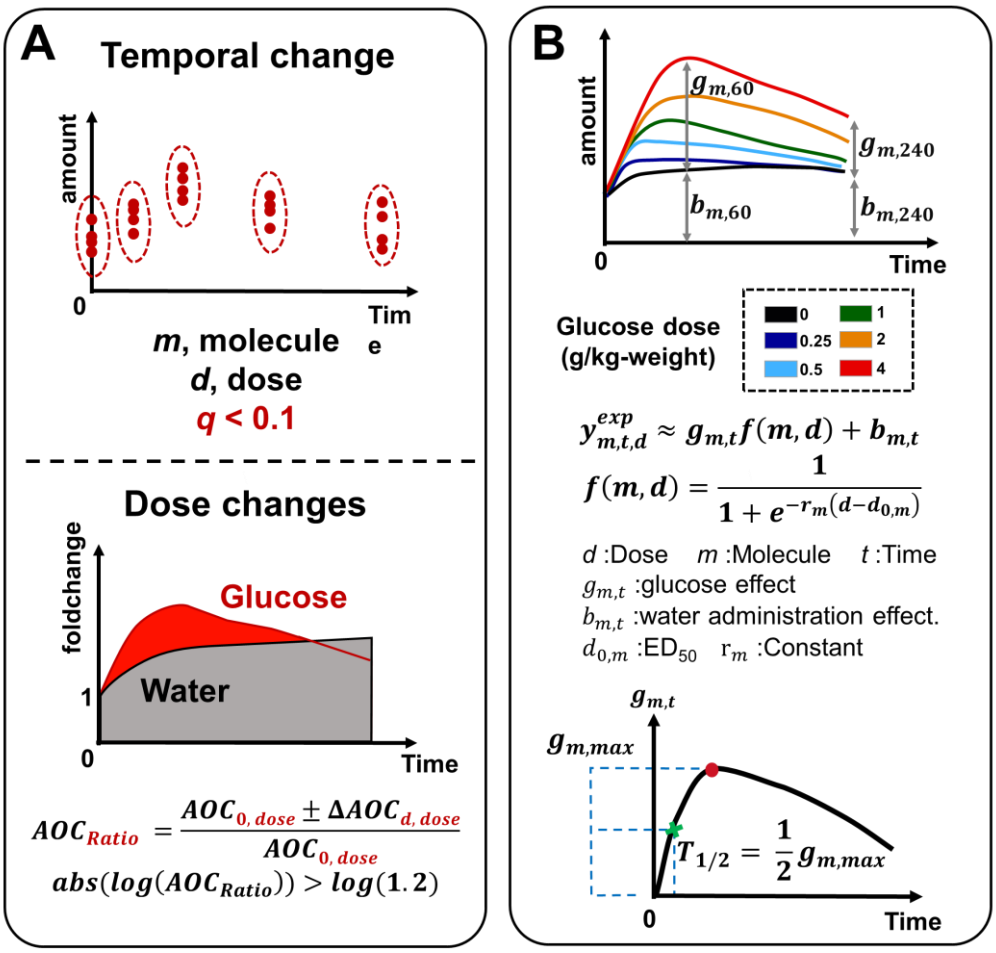

Supplementary Figure 1. Identification of dose-dependent glucose-responsive molecules and their glucose-responsiveness indicators for dose sensitivity and response time

(A) Definition of dose-dependent glucose-responsive molecules using AOC ratio and FDR-adjusted P value (q value). *q value < 0.1 and absolute $\log_{10}$AOC ratio > 0.079 ($\log_{10}1.2$).
(B) Method for the estimation of indicators: ED_{50}, an index of sensitivity to glucose doses, and $T_{1/2}$, an index of response time.

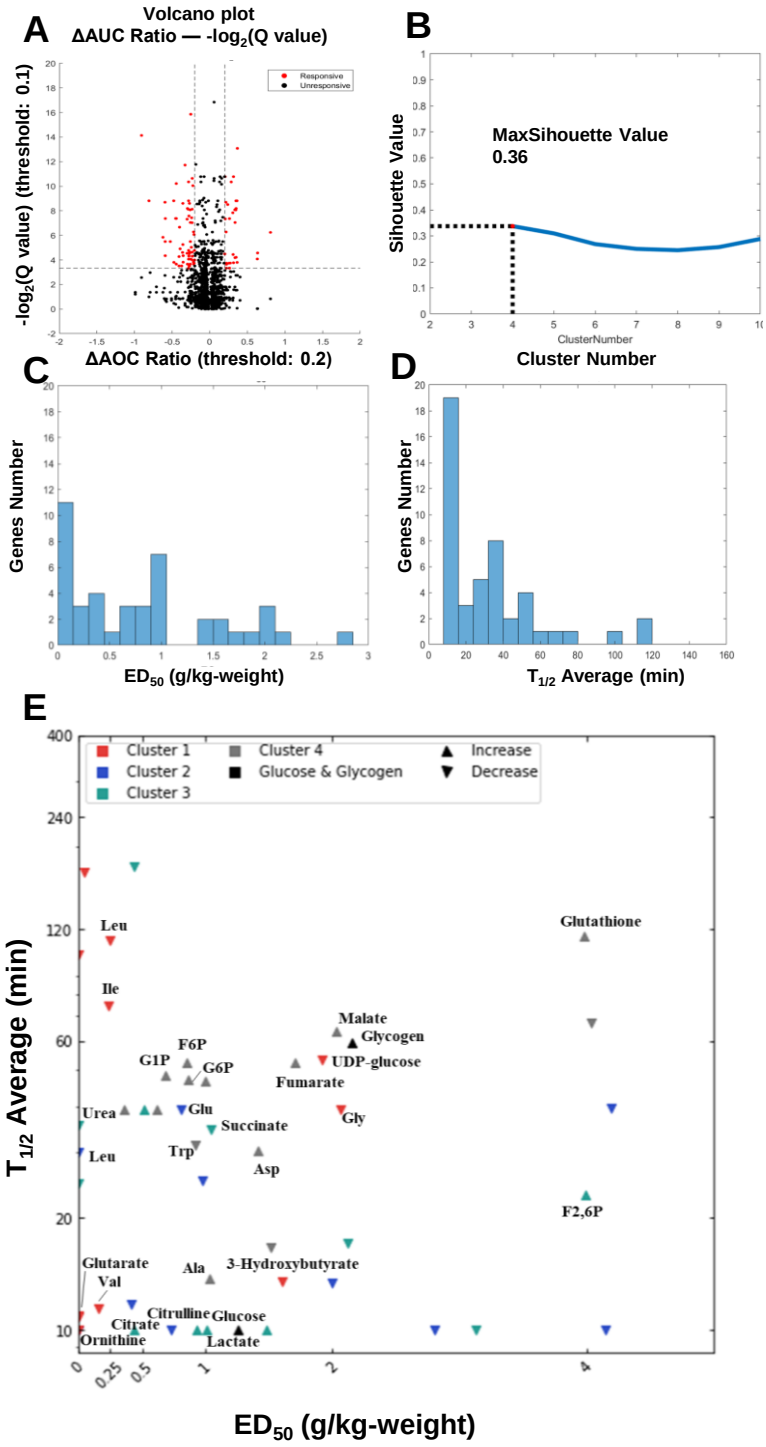

Supplementary Figure 2. Contents of the identification of dose-dependent glucose-responsive metabolites. Related to Figure 2.

(A) Volcano plot for q value (vertical axis) and foldchange (horizonal axis) of dose-dependent glucose-responsive metabolites in all doses. The q value threshold of 0.1 and foldchange threshold of 0.2 are indicated as dashed lines. Red dots exhibited dose-dependent glucose-responsive metabolites in a specific glucose or water dose.
(B) Line plot of Silhouette values of different cluster numbers for dose-dependent glucose-responsive metabolites
(C) Histogram of ED_{50} values of dose-dependent glucose-responsive metabolites
(D) Histogram of $T_{1/2}$ values of dose-dependent glucose-responsive metabolites
(E) Scatter plot exhibited the distribution of ED_{50} (horizonal axis) and $T_{1/2}$ (vertical axis) for dose-dependent glucose-responsive genes and phosphorylation of insulin signaling molecules. The directions of the scatter marks represented their responsive patterns (up: increase, down: decrease). The colors of the scatter marks represented the clustering result of these metabolites. Black scatter marks represented dose-dependent glucose-responsive phosphorylation of insulin signaling molecules.

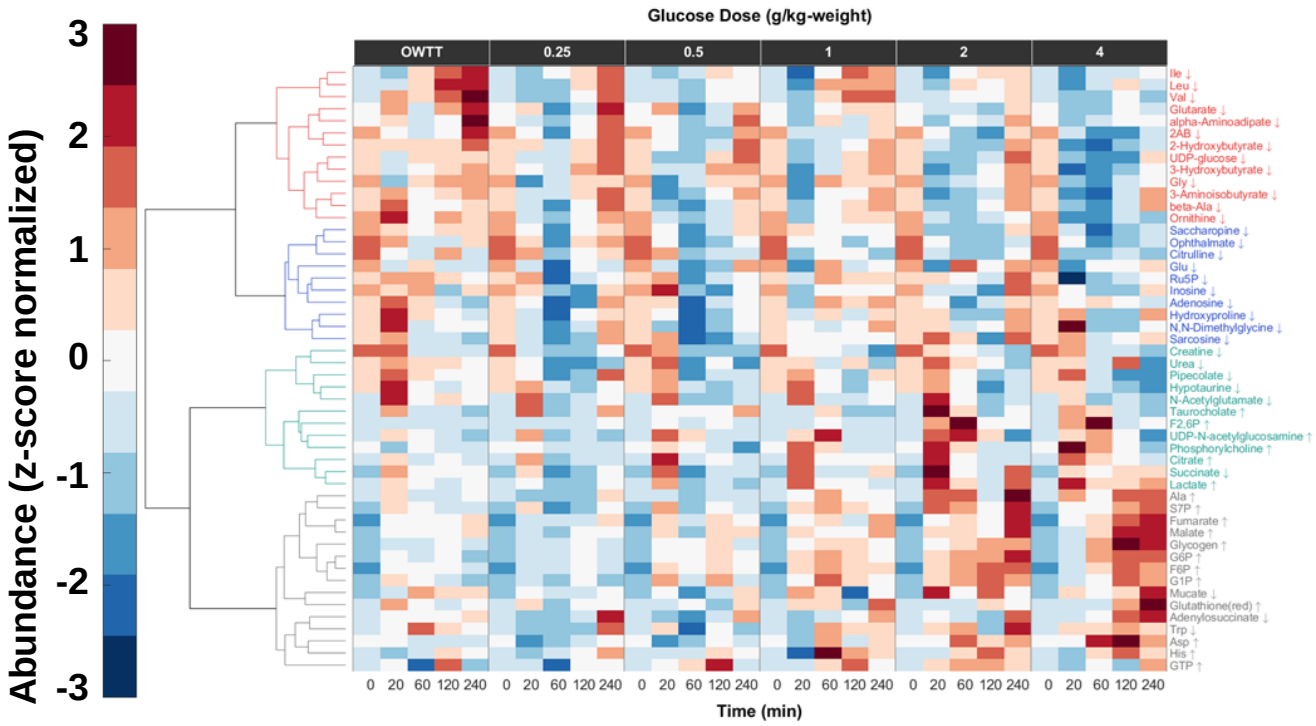

Supplementary Figure 3. The time courses of dose-dependent glucose-responsive metabolites from the livers after six doses of oral glucose administration (n = 5 mice per dose at all time points). Six time courses for each gene were z-score normalized. Metabolites were ordered by hierarchical clustering using Euclidean distance and Ward's method. The colors of the dendrogram and metabolites names represented the clustering results (Red: Cluster 1, Blue: Cluster 2, Red: Cluster 3, Cyan: Cluster 3, Grey: Cluster 4). The arrow after the metabolite names represented the responsive patterns (Up arrow: Increase, Down arrow: Decrease).

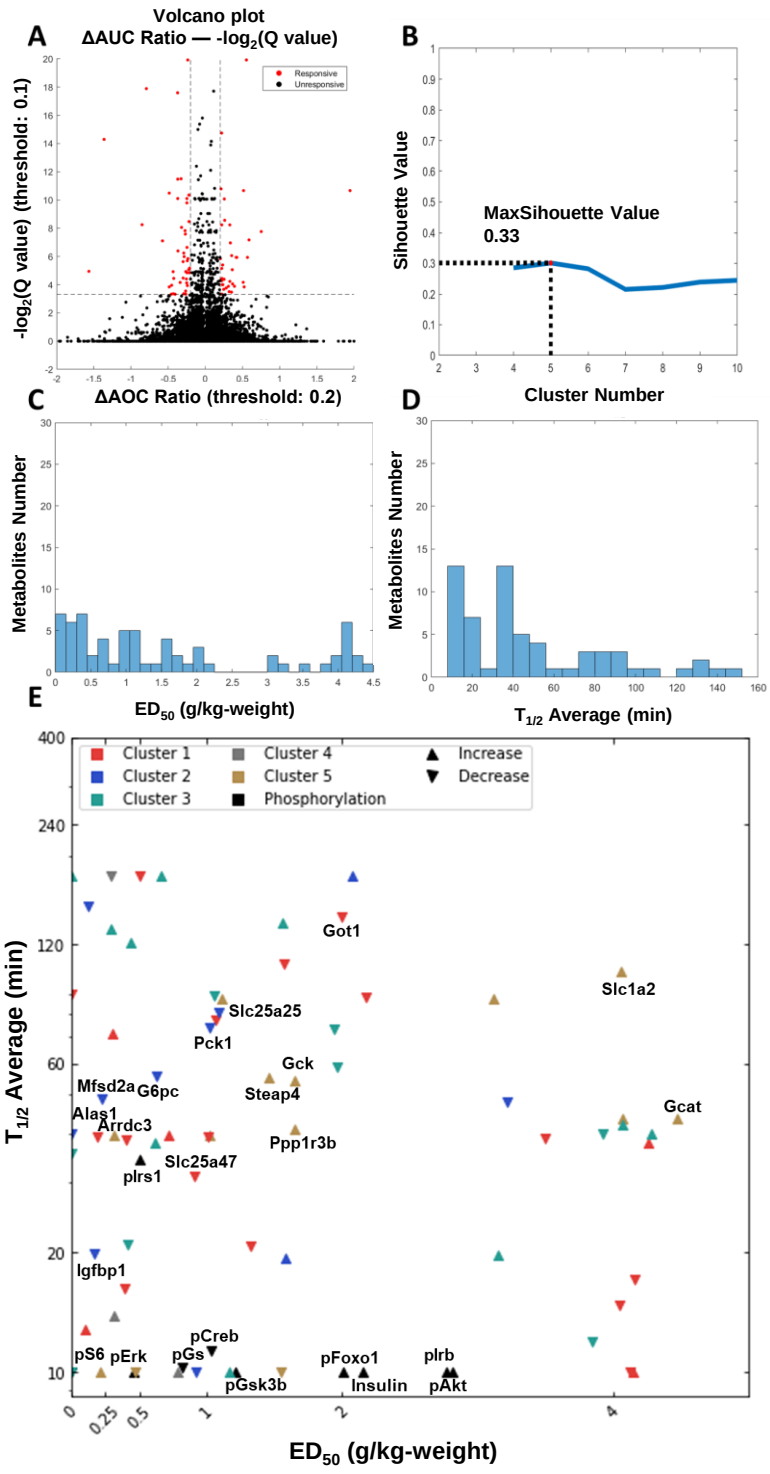

Supplementary Figure 4. Contents of the identification of dose-dependent glucose-responsive genes and insulin signaling molecules. Related to Figure 3.

(A) Volcano plot for q value (vertical axis) and foldchange (horizonal axis) of dose-dependent glucose-responsive gene expressions in all doses. The q value threshold of 0.1 and foldchange threshold of 0.2 are indicated as dashed lines. Red dots exhibited dose-dependent glucose-responsive gene expressions in a specific glucose or water dose.

(B) Line plot of Silhouette values of different cluster numbers for dose-dependent glucose-responsive gene expressions

(C) Histogram of ED_{50} values of dose-dependent glucose-responsive gene expressions

(D) (D) Histogram of T1/2 values of dose-dependent glucose-responsive gene

(E) expressions

(F) (E) Scatter plot exhibited the distribution of

(G) ED50 (horizonal axis) and T1/2 (vertical axis) for dose-dependent glucose-responsive gene expressions and phosphorylation of insulin signaling molecules. The directions of the scatter marks represented their responsive patterns (up: increase, down: decrease). The colors of the scatter marks represented the clustering result of these metabolites. Black scatter marks represented dose-dependent glucose-responsive phosphorylation of insulin signaling molecules.

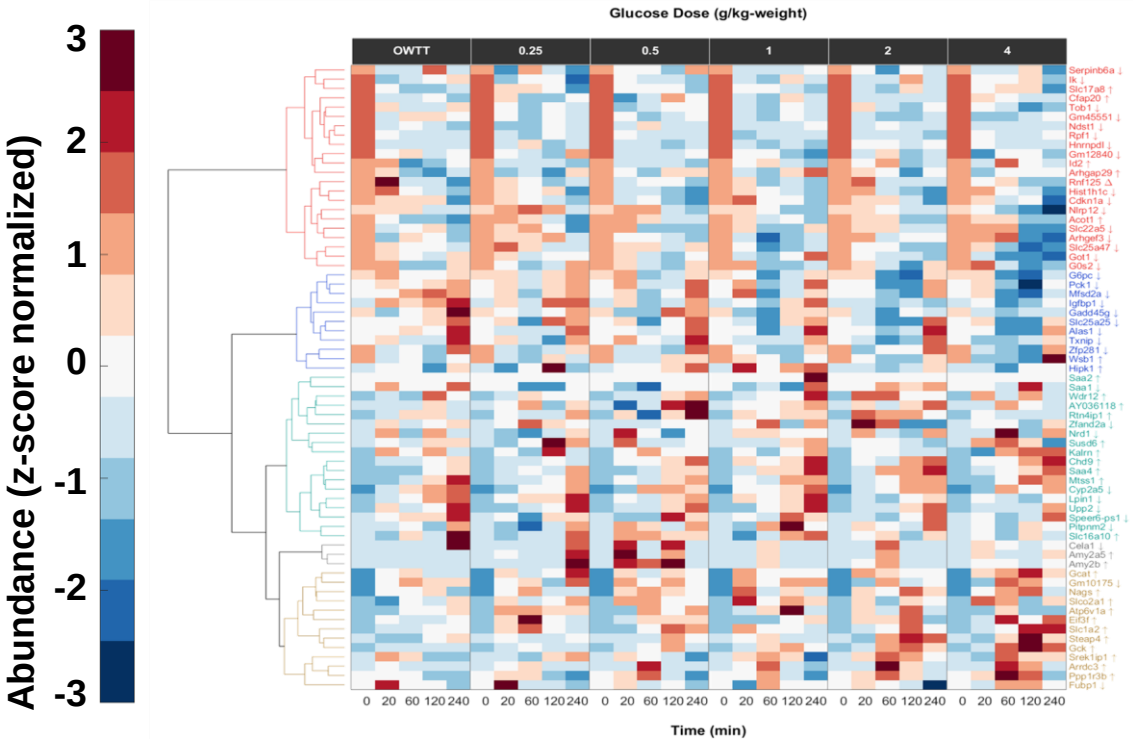

Supplementary Figure 5. The time courses of dose-dependent glucose-responsive genes from the livers after six doses of oral glucose administration (n = 5 mice per dose at all time points). Six timecourses for each gene were z-score normalized. Genes were ordered by hierarchical clustering using Euclidean distance and Ward's method. The colors of the dendrogram and gene names represented the clustering results (Red: Cluster 1, Blue: Cluster 2, Red: Cluster 3, Cyan: Cluster 3, Grey: Cluster 4, Gold: Cluster 5). The arrow after the gene names represented the responsive patterns (Up arrow: Increase, Down arrow: Decrease, triangle: Ambiguous).

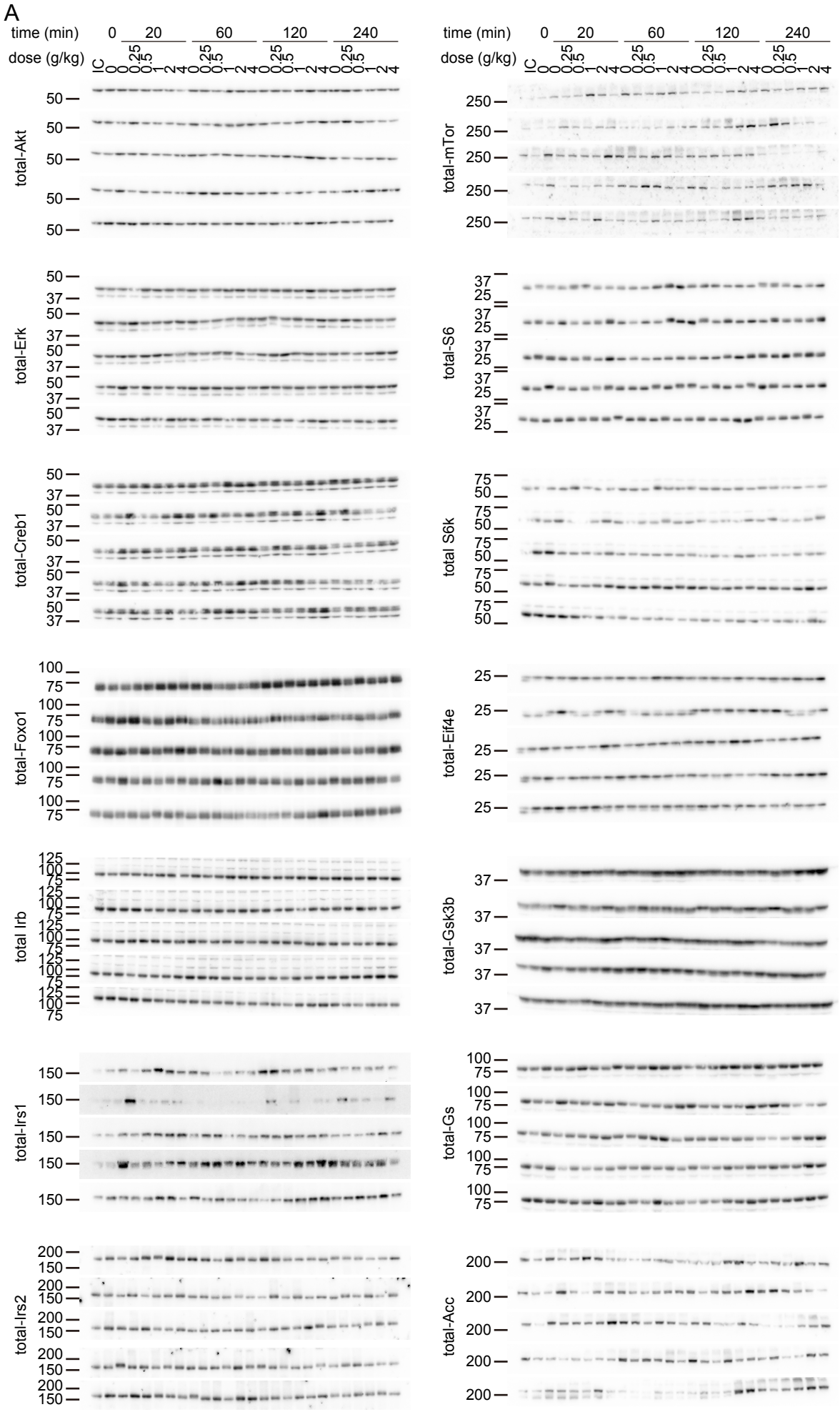
A
time (min)
0
20
60
120
240
dose (g/kg)
IC
0.25
0.5
1
2
4
total-Akt
total-Erk
total-Creb1
total-Foxo1
total Irb
total-Irs1
total-Irs2
total-mTor
total-S6
total S6k
total-Eif4e
total-Gsk3b
total-Gs
total-Acc

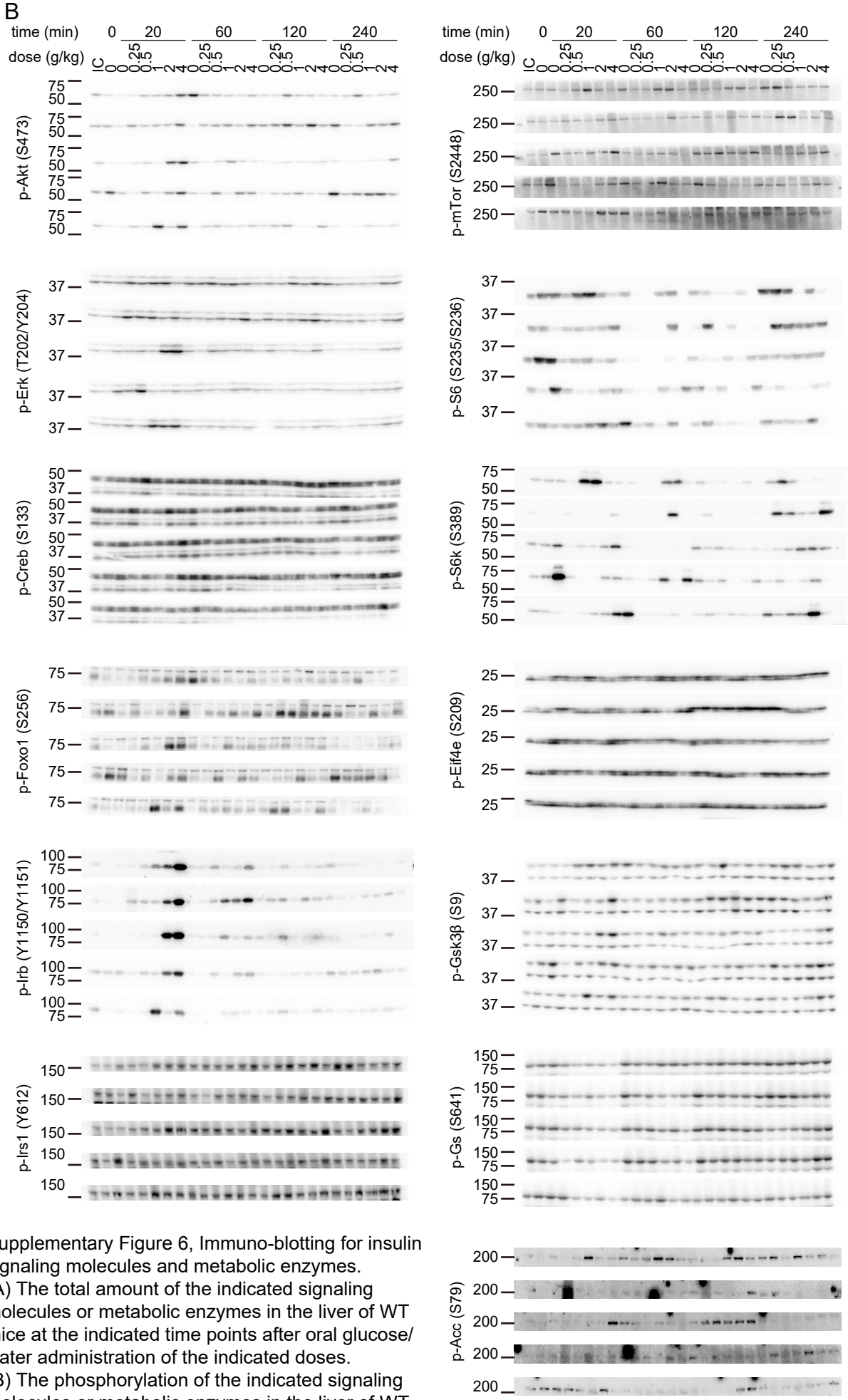

Supplementary Figure 6, Immuno-blotting for insulin signaling molecules and metabolic enzymes.
(A) The total amount of the indicated signaling molecules or metabolic enzymes in the liver of WT mice at the indicated time points after oral glucose/ water administration of the indicated doses.
(B) The phosphorylation of the indicated signaling molecules or metabolic enzymes in the liver of WT mice at the indicated time points after oral glucose/ water administration of the indicated doses. IC stands for internal control to normalize the data of different membranes.

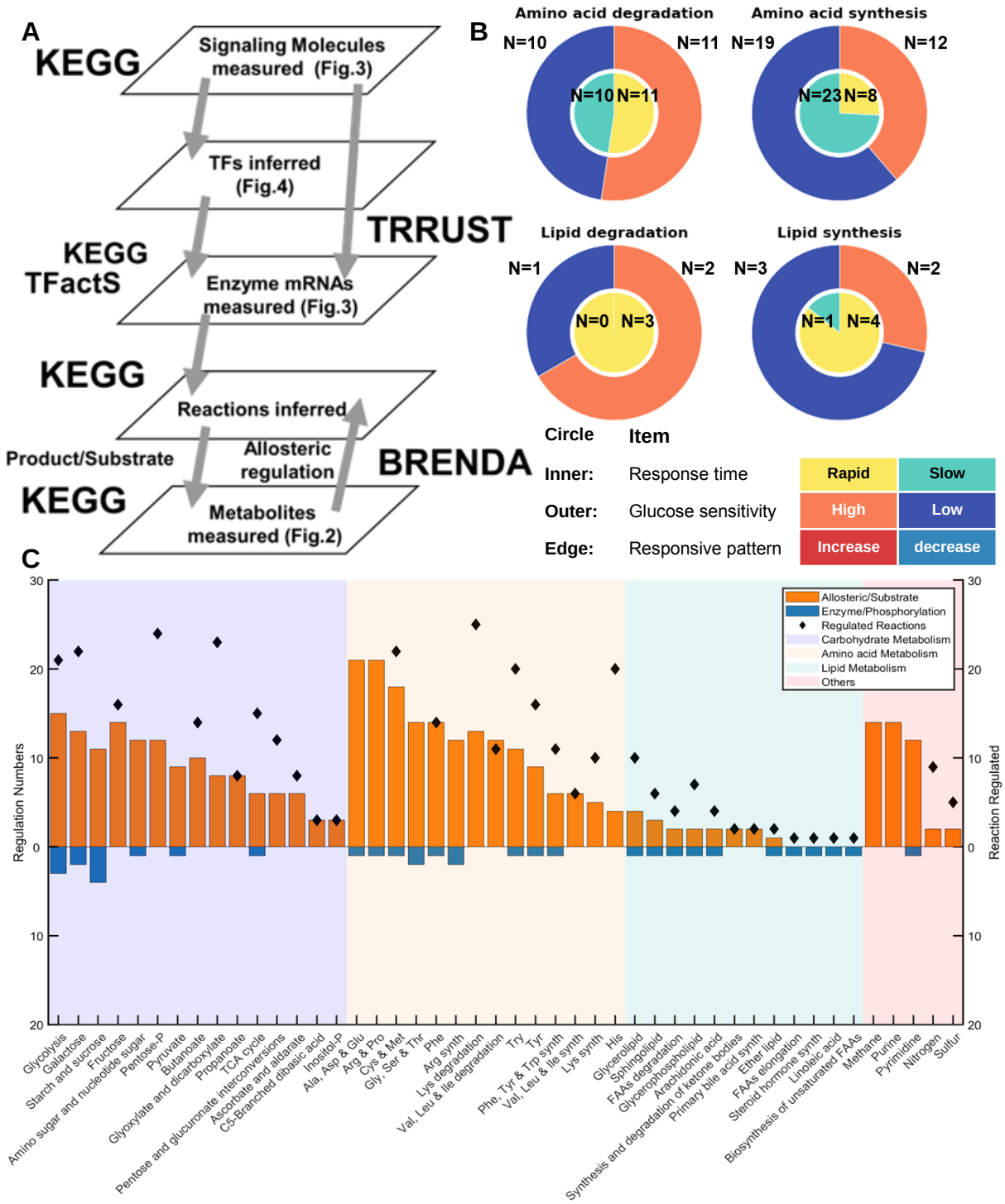

Supplementary Figure 7. Contents of the construction of dose-dependent glucose metabolic transomics network.

(A) The procedure for constructing the regulatory transomics network for dose-dependent glucose-responsive metabolic reactions. The insulin signal, transcription factor (TF), enzyme, and metabolite layers correspond to dose-dependent glucose-responsive molecules. The reaction layer represents reactions in the KEGG reaction database and are regulated by glucose-responsive molecules. The upward and downward arrows indicate interlayer regulatory connections. The databases used to identify the interlayer regulatory connections are shown on the arrows.

(B) Number of dose-dependent glucose-responsive reactions in each KEGG pathway from carbohydrate metabolism, energy metabolism, lipid metabolism, nucleotide metabolism and amino acid metabolism. Orange bars represent the number of allosteric or substrate regulations and blue bars represent enzyme or phosphorylation regulations connected to reactions in these pathways. Diamond scatters are the number of the reactions regulated in each pathway. Background color represent the type of metabolism these pathways are from: Blue, carbohydrate metabolism; Yellow, amino acid metabolism; Green, lipid metabolism; Red, other types of metabolism.

(C) The glucose responsiveness of response time and glucose sensitivities for amino acid and lipid degradation and synthesis pathways according to KEGG database. The color of the inner circle of nodes representing the response time of the share of classified response time that connected to a specific type of pathway (Yellow, rapid; Aquamarine, slow). The color of the outer circle of nodes representing the glucose sensitivity of the share of classified glucose sensitivity that connected to a specific type of pathway (Orange, high glucose sensitivity; Blue, low glucose sensitivity).

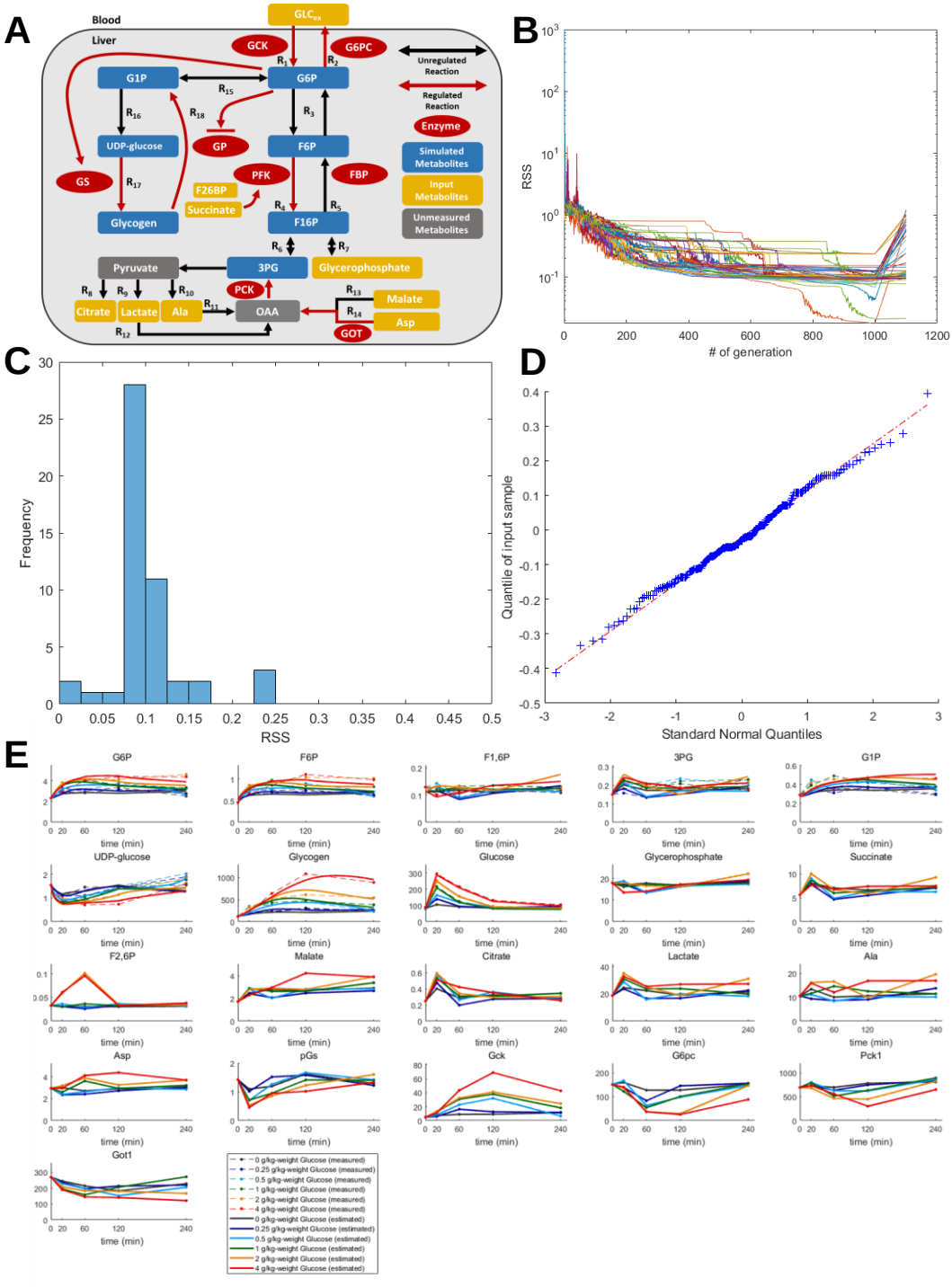

Supplementary Figure 8. The metabolic network and simulation results for the *in silico* fluxes estimation

(A) The metabolic network used for kinetic modeling. Molecules in blue boxes represented fitted metabolites. Molecules in yellow boxes represented input metabolites and molecules in grey boxes represented simplified metabolites that were not measured. Arrows represented unregulated metabolic reactions (black) or regulated metabolic regulations (red). Molecules in red boxes represented metabolic regulators.

(B) Line plot of best-fitted RSS value (y axis) with number of generations (x axis) simulated in the 50 iterations

(C) Histogram of RSS values simulated in the 50 iterations

(D) Quantile-quantile plot of residual data (y axis) versus standard normal quantiles (x axis)

(E) Time courses of simulated or input molecule amounts (solid lines) versus the experimentally measured time course for simulated metabolites (dashed lines)

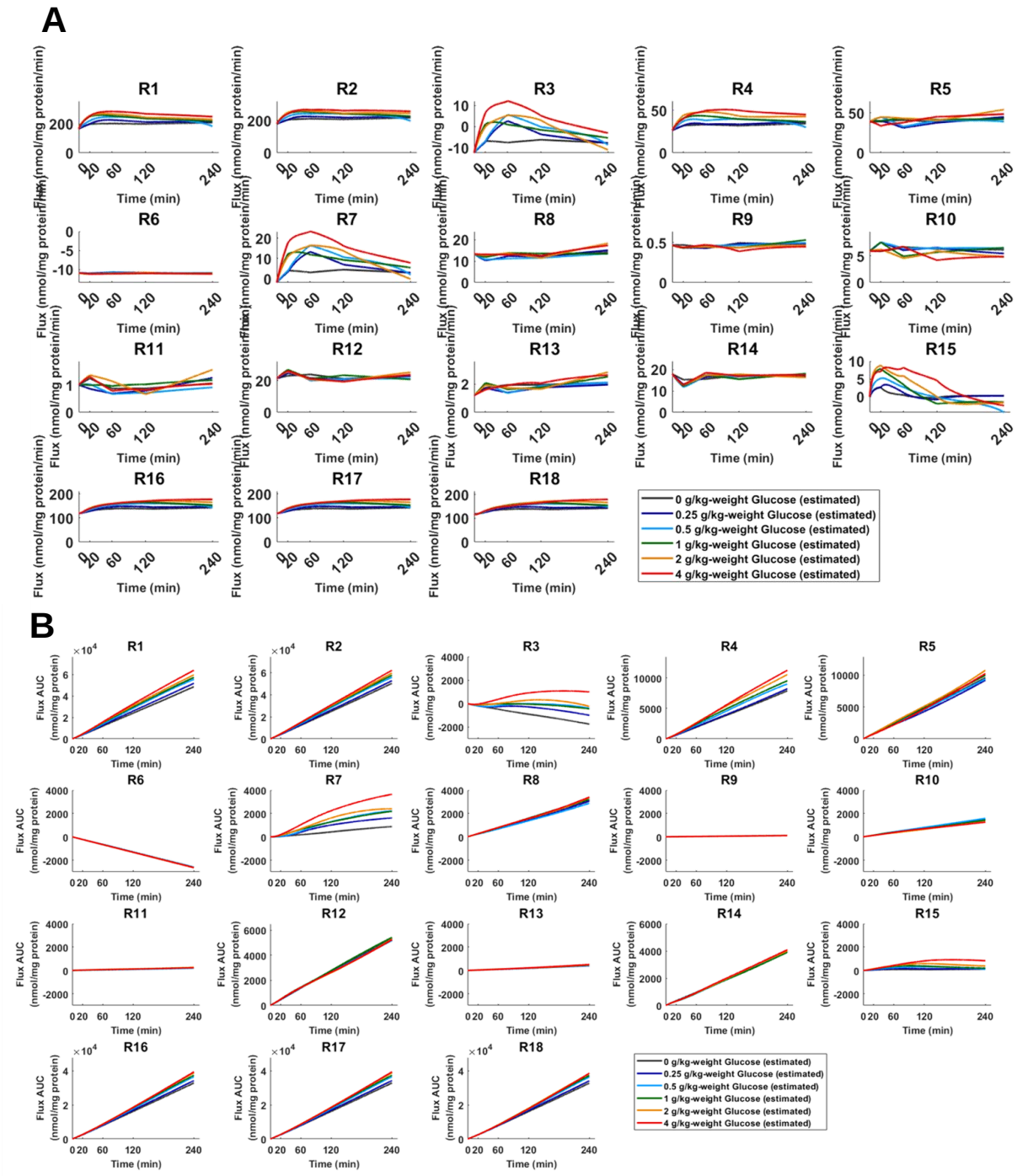

Supplementary Figure 9. Timecourse of simulated reaction fluxes and flux AOCs

(A) The time courses of simulated reaction fluxes for the modeled metabolic network.

(B) The time courses of simulated reaction flux AOCs for the modeled metabolic network.

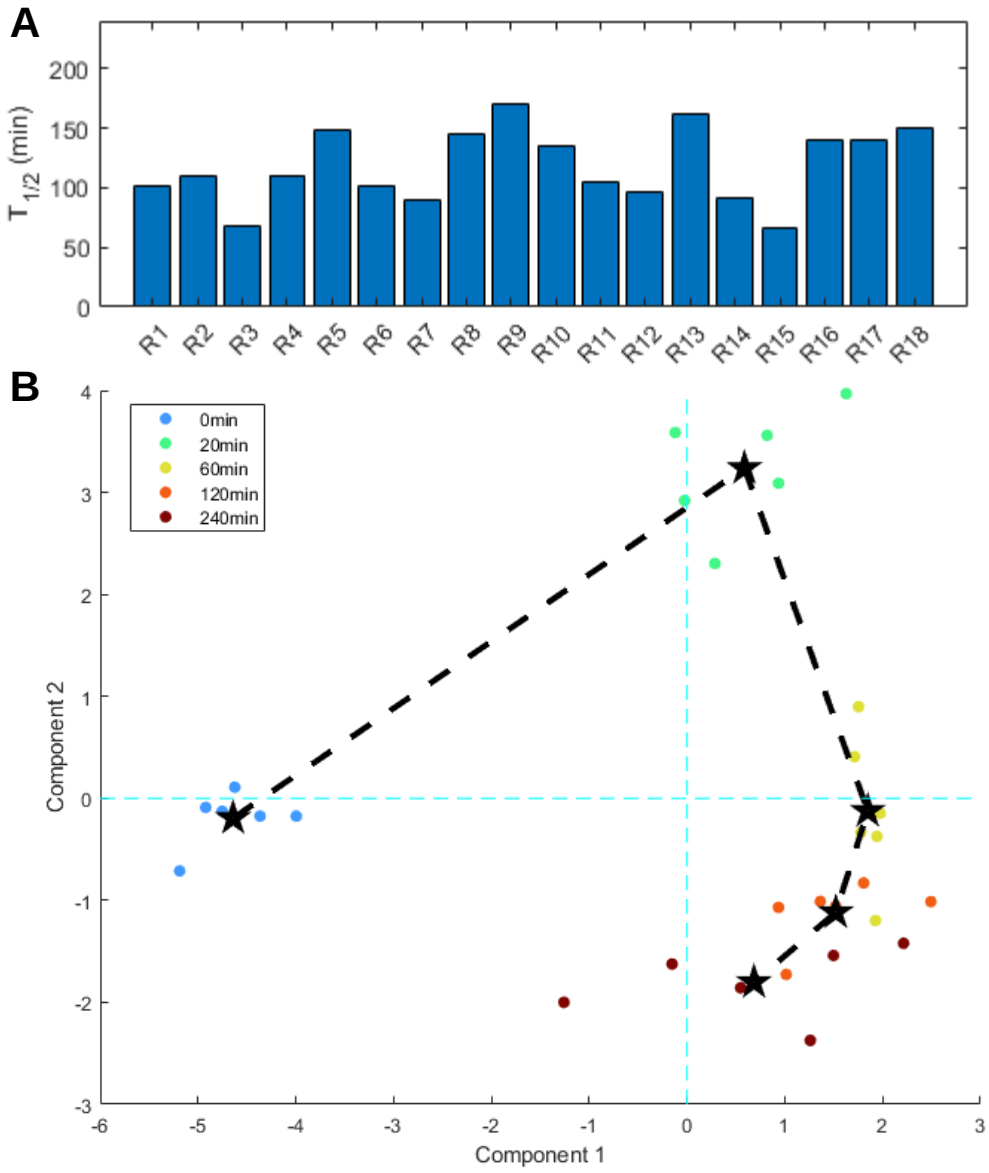

Supplementary Figure 10. Contents of response time of estimated flux AOCs and the PCA results for the staging of time points for estimated fluxes related to figure 7.

(A) Bar plot of $T_{1/2}$s for simulated flux AOCs.
(B) Scores for the top 2 components in the principal component analysis (PCA) results of normalized fluxes time course. Dashed black line indicates the time course of mean values in component 1 and 2 for each time point. Dashed cyan line showed the four quadrants divided by the 0 value of component 1 and 2. Mean values of component 2 for the timepoints of 0 and 60 min were along 0

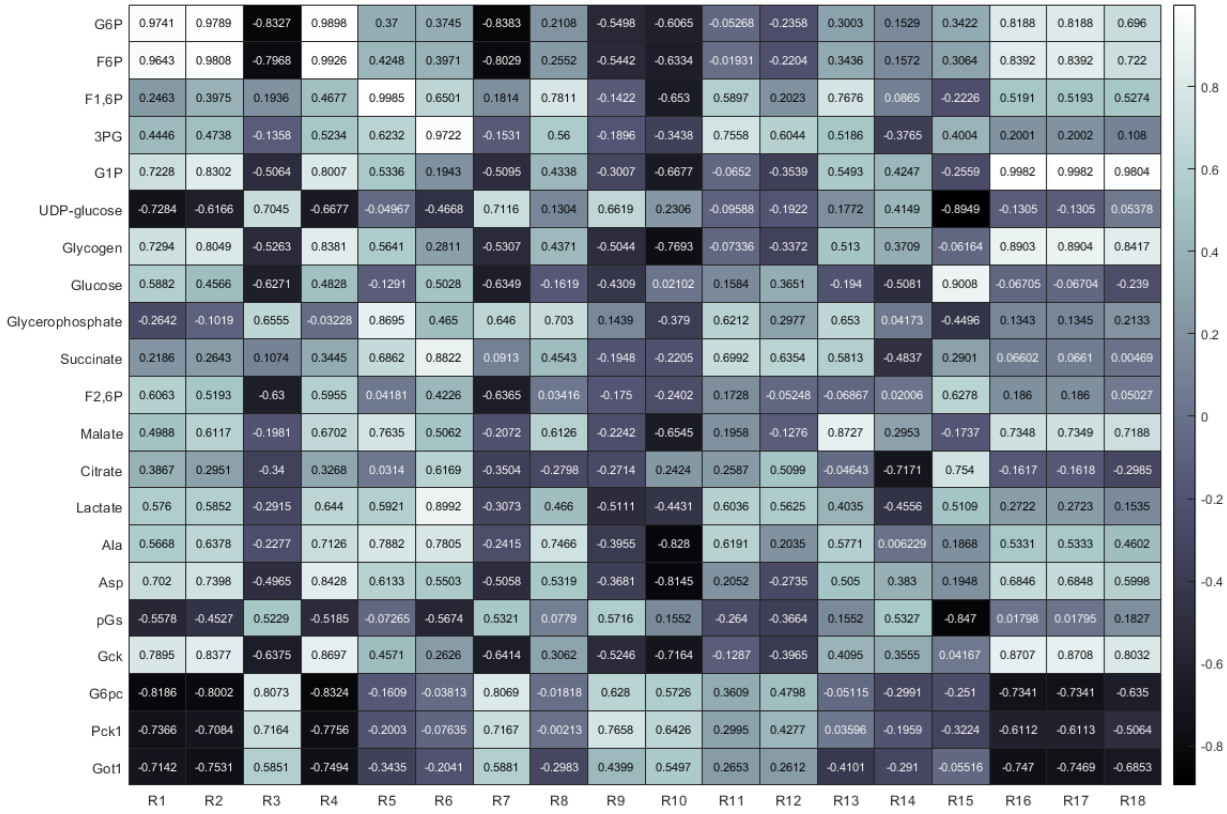

Supplementary Figure 11. Heatmap of Pearson correlations coefficients between the time course of estimated fluxes and measured molecules

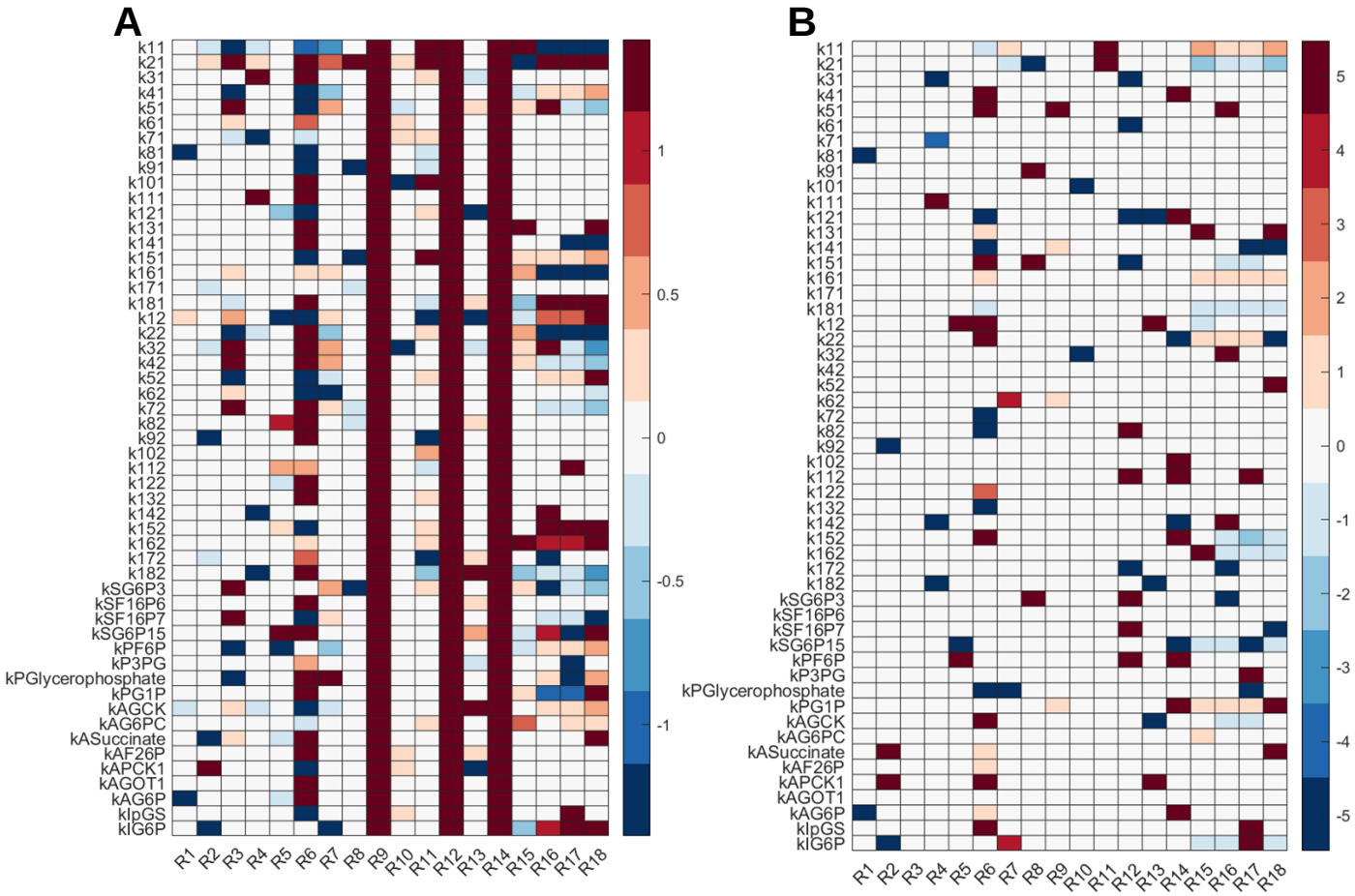

Supplementary Figure 12. Sensitivity analysis for estimated metabolic fluxes on parameters

(A) Heatmap of parameter sensitivity analysis on the ED_{50} for estimated metabolic fluxes

(B) Heatmap of parameter sensitivity analysis on the $T_{1/2}$ for estimated metabolic fluxes

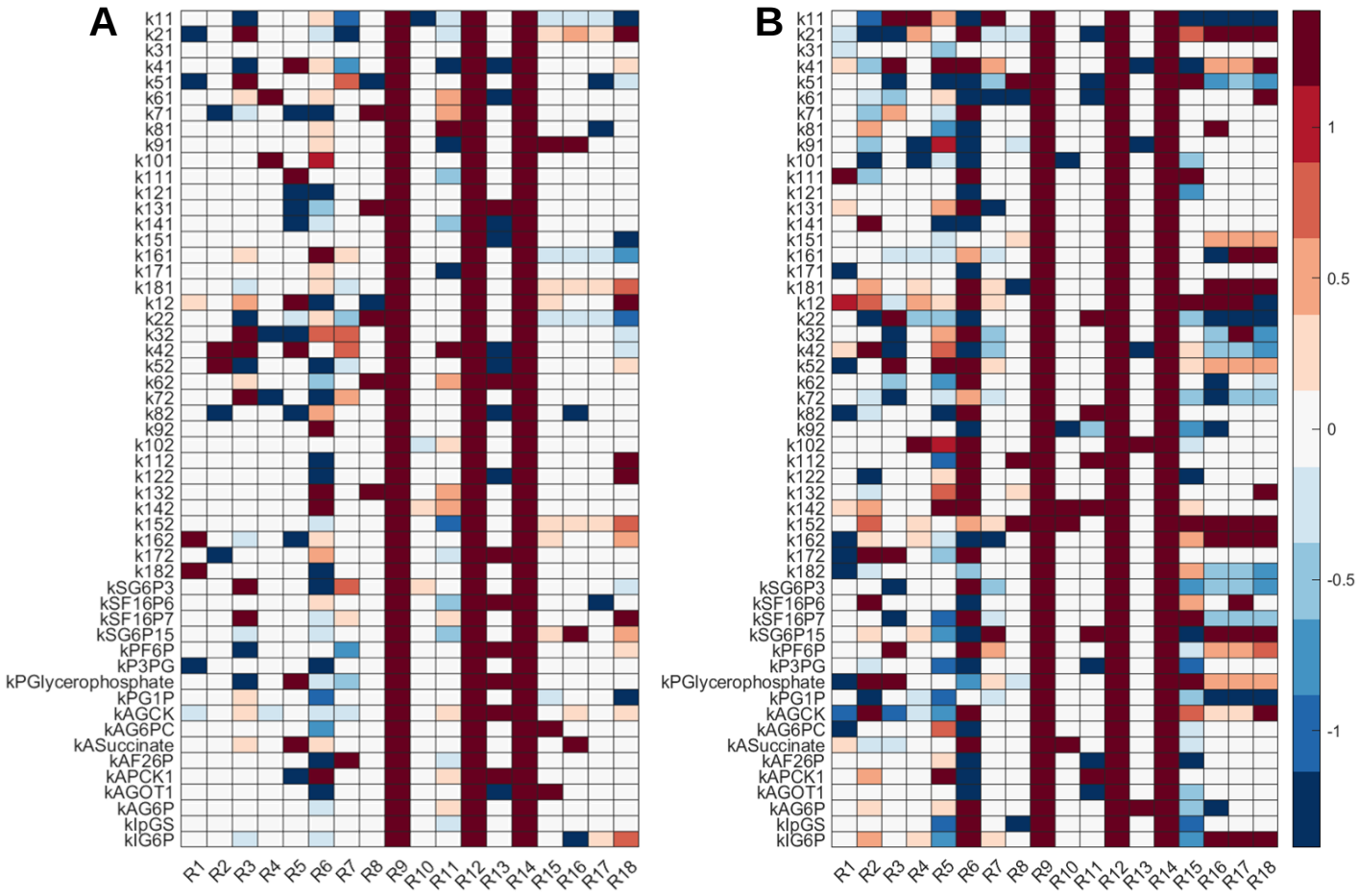

Supplementary Figure 13. Sensitivity analysis for estimated metabolic fluxes on parameters in two phases

(A) Heatmap of parameters sensitivity of flux ED_{50}s during 0-60min

(B) Heatmap of parameters sensitivity of flux ED_{50}s during 60-240min

p-Akt (S473)

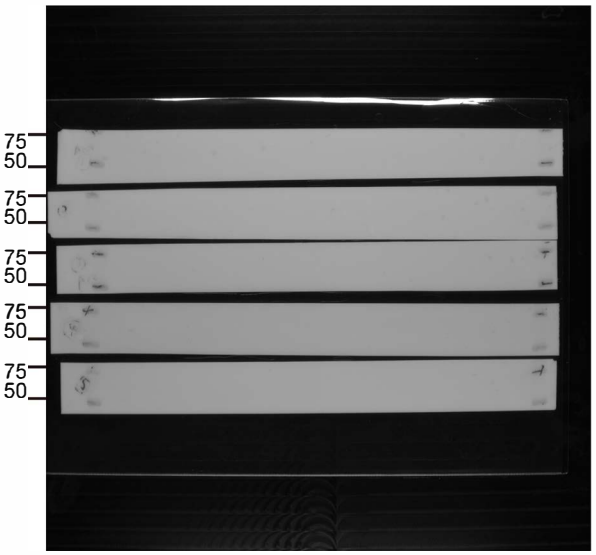

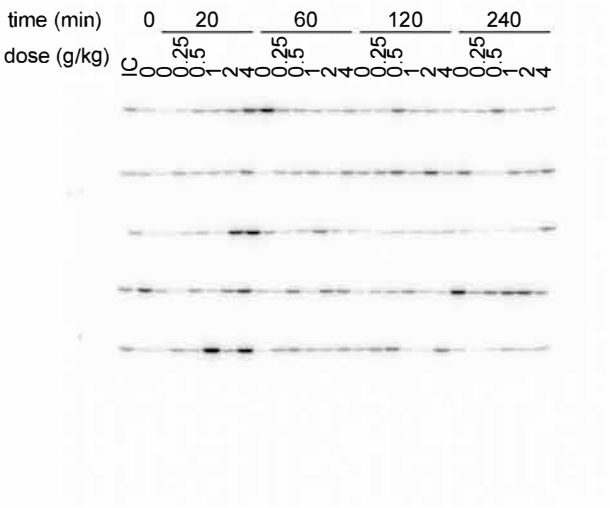

p-Erk (T202/Y204)

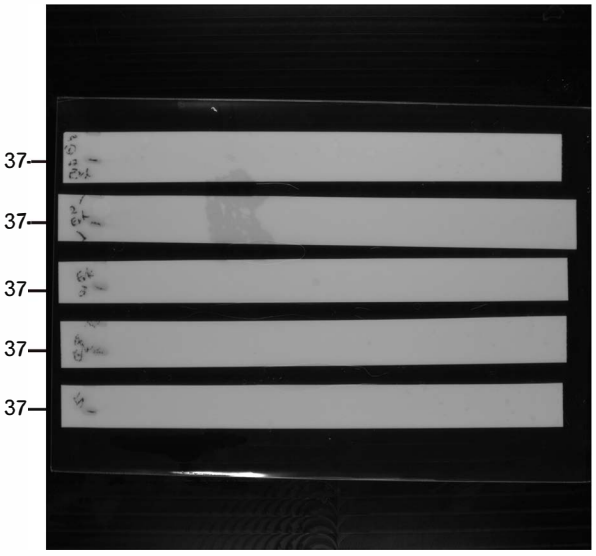

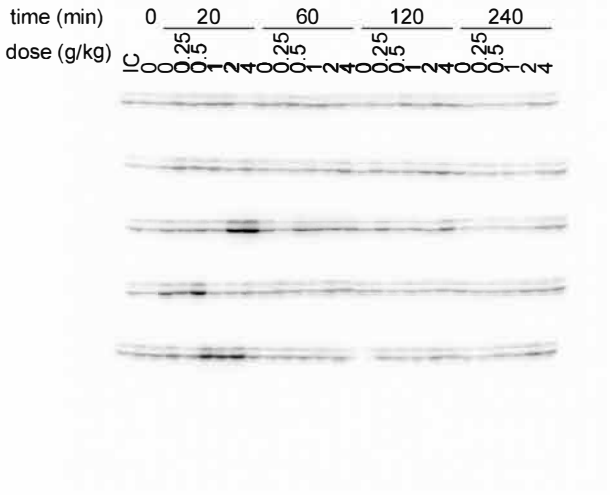

p-Creb (S133)

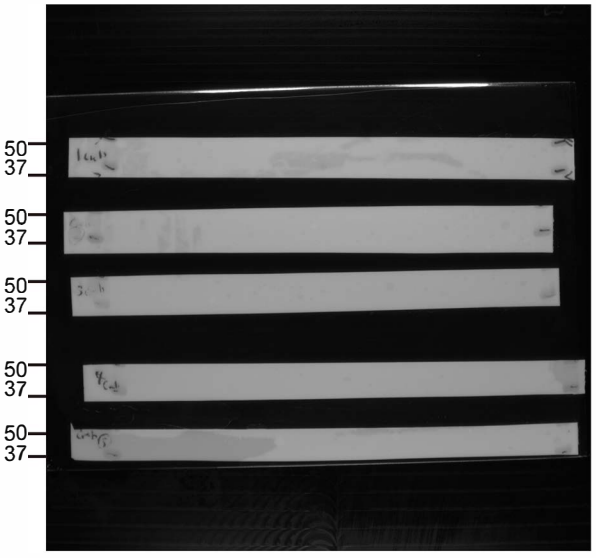

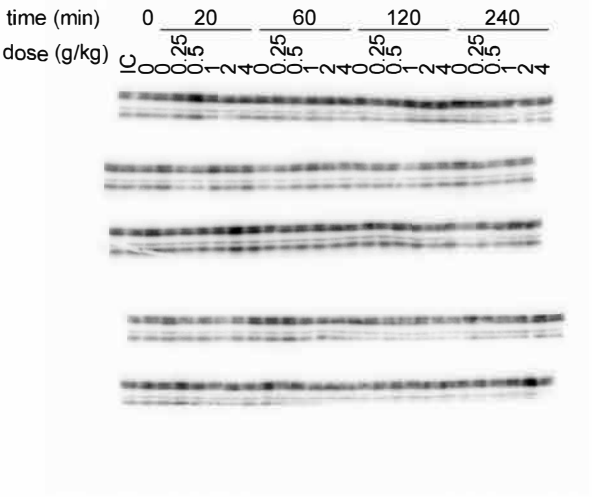

p-Foxo1 (S256)

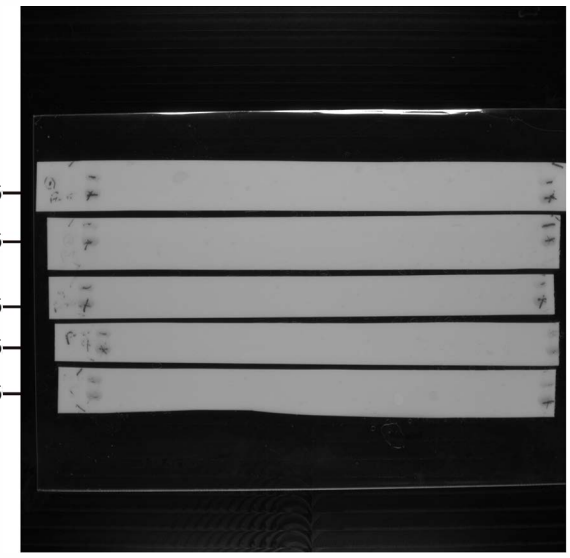

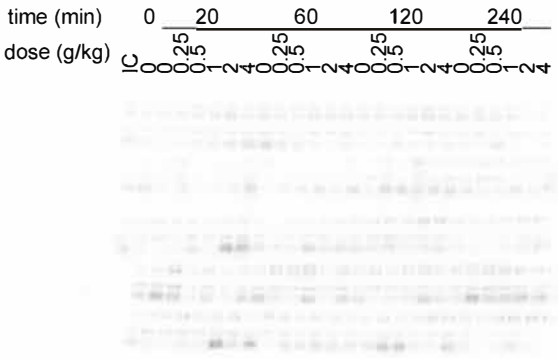

p-Irb (Y1150/Y1151)

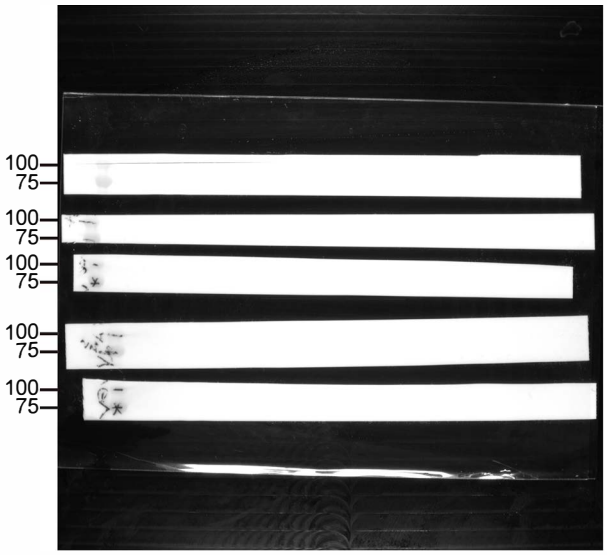

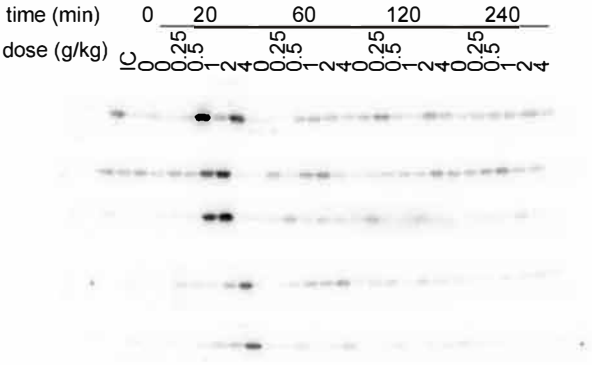

*The order of the membranes were opposite to the Fig. S6

p-Irs1 (Y612)

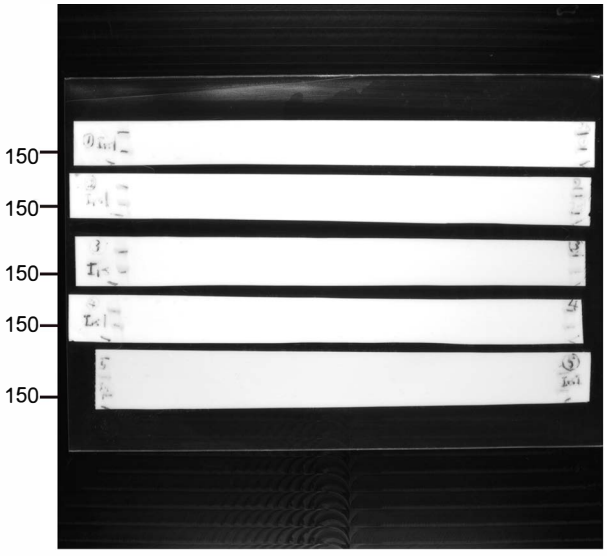

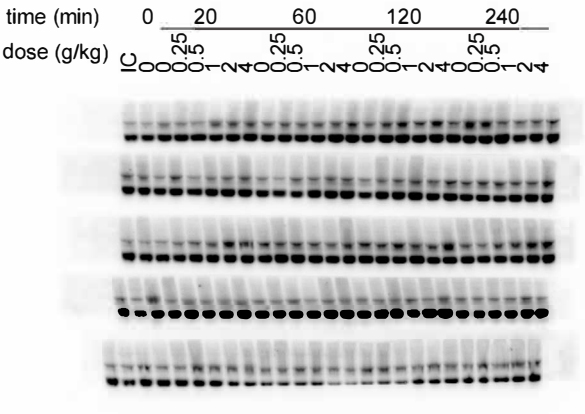

p-mTor (S2448)

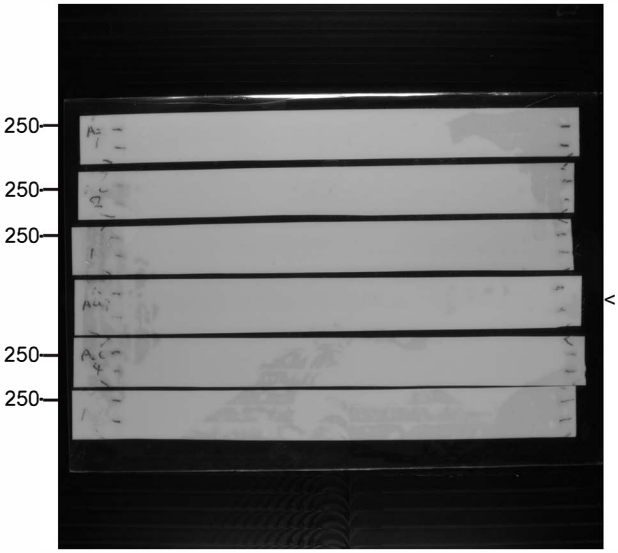

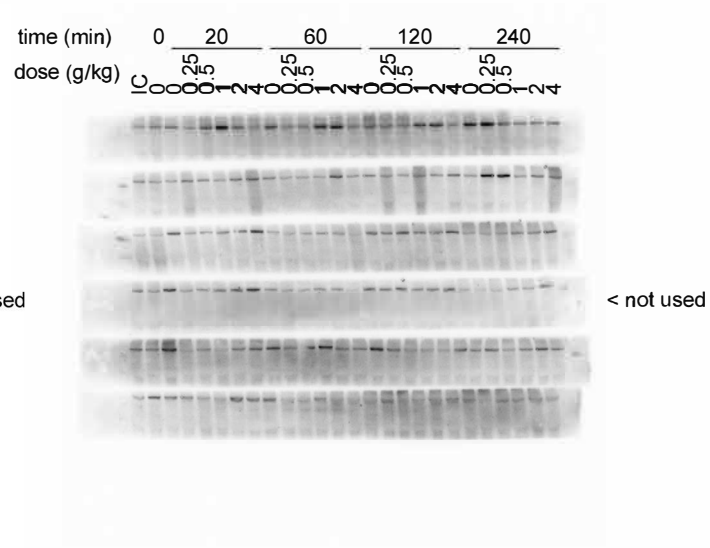

p-S6 (S235/S236)

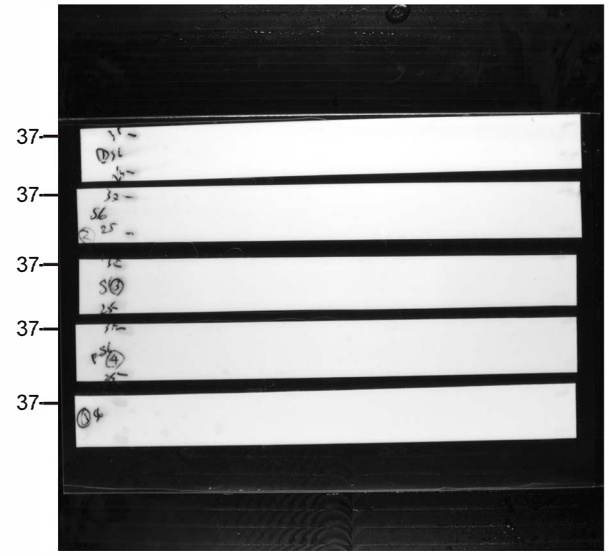

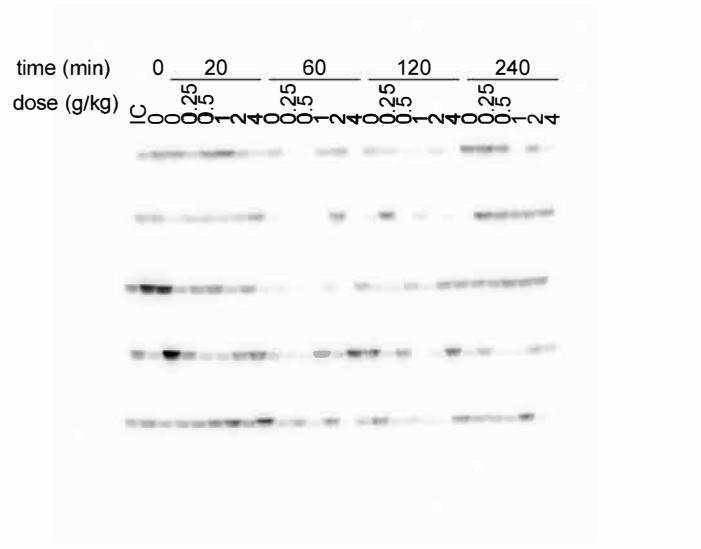

p-S6k (S389)

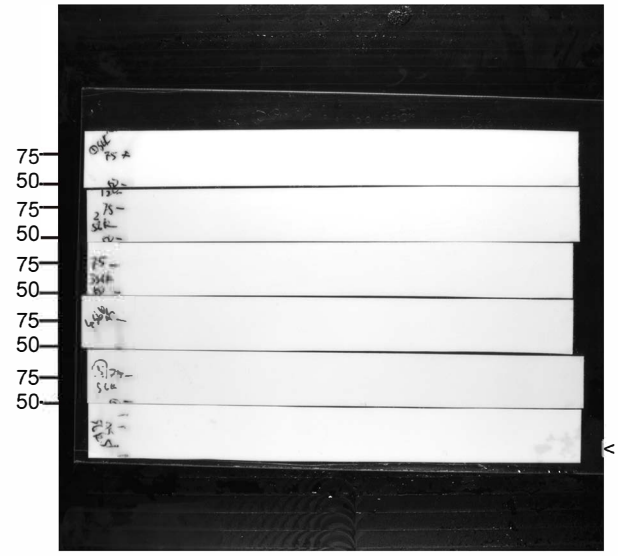

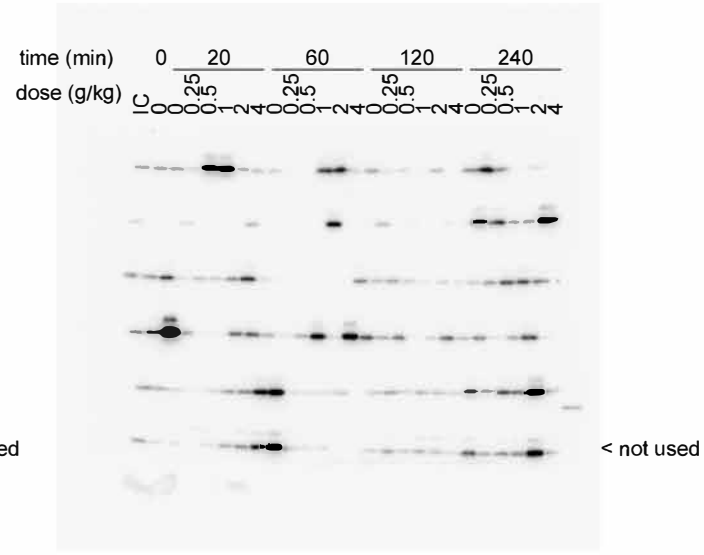

p-Eif4e (S209)

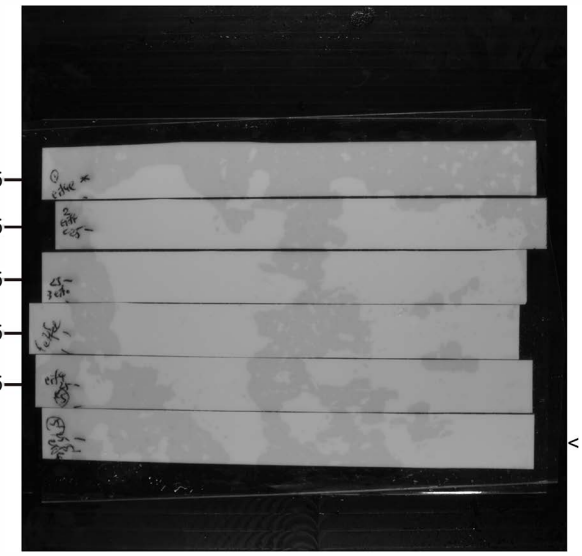

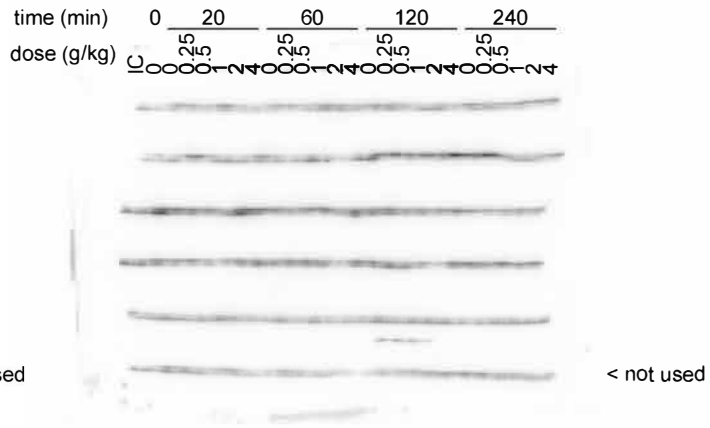

p-Gsk3β (S9)

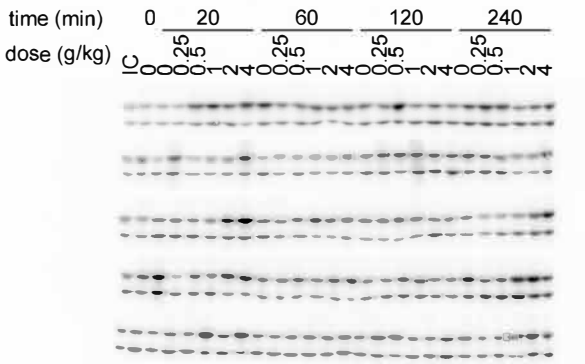

p-Gs (S641)

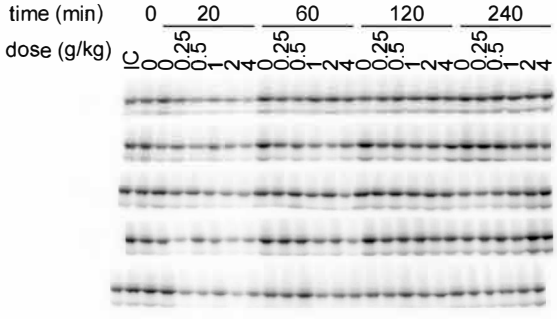

p-Acc (S79)

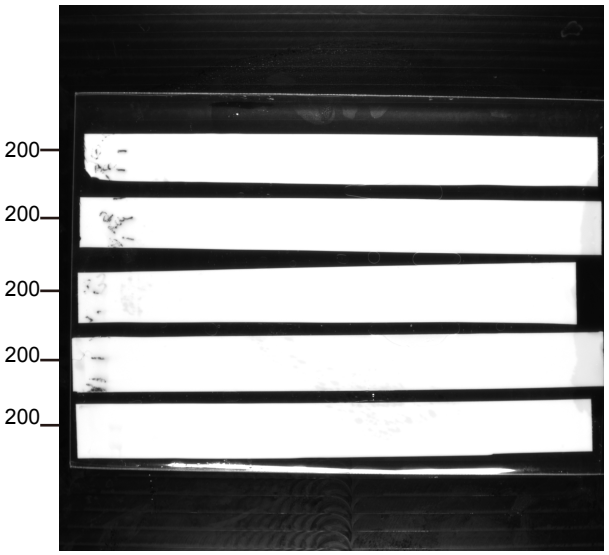

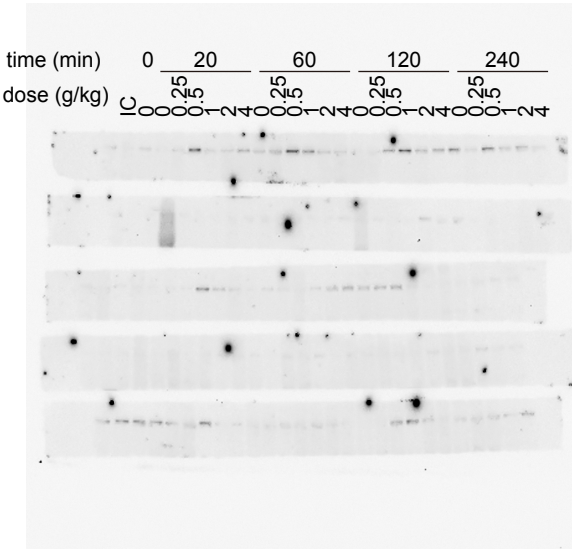

total-Akt

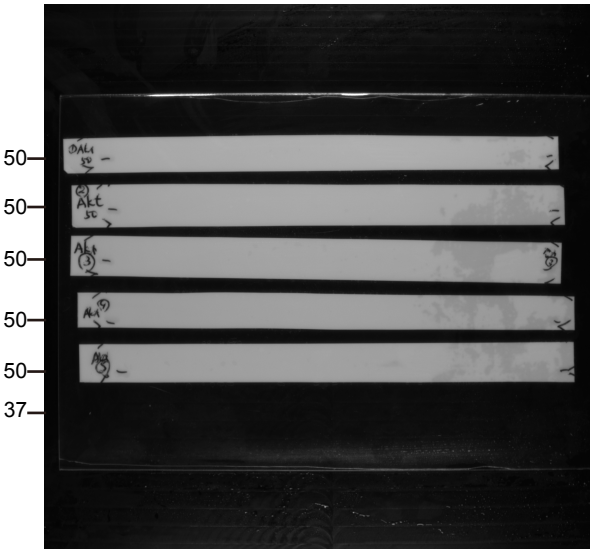

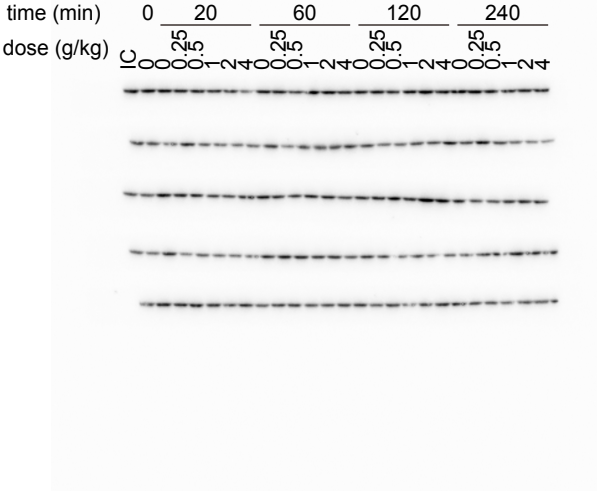

total-Erk

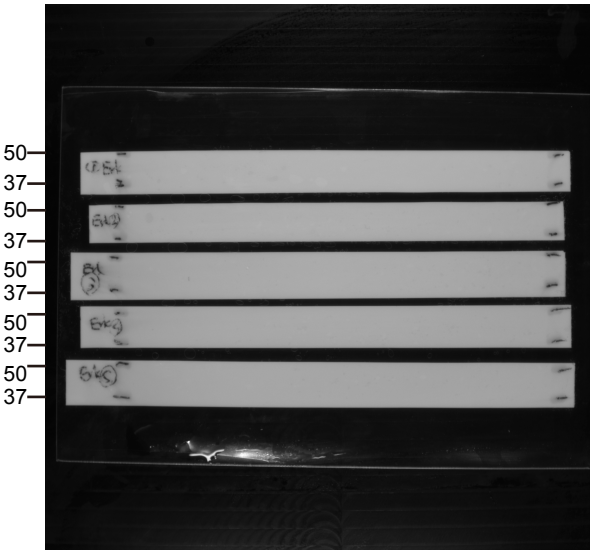

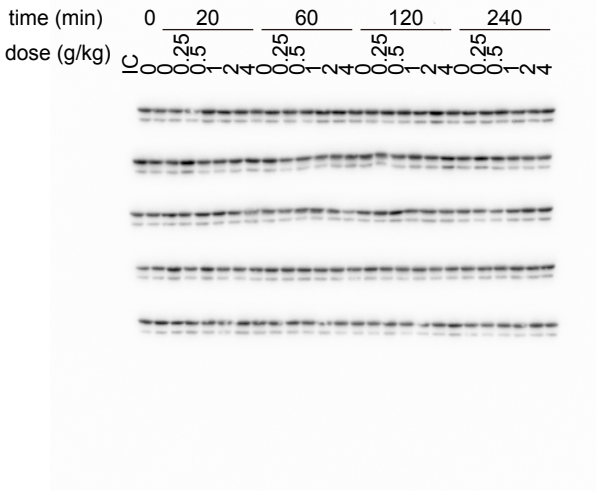

total-Creb1

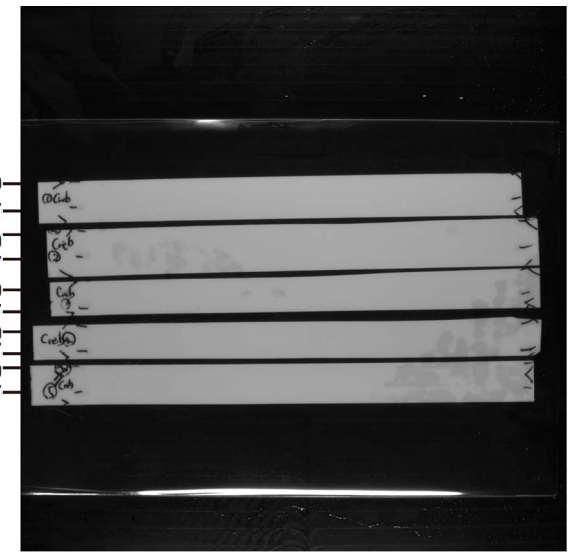

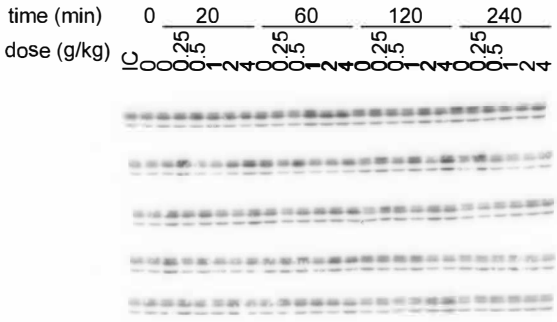

total-Foxo1

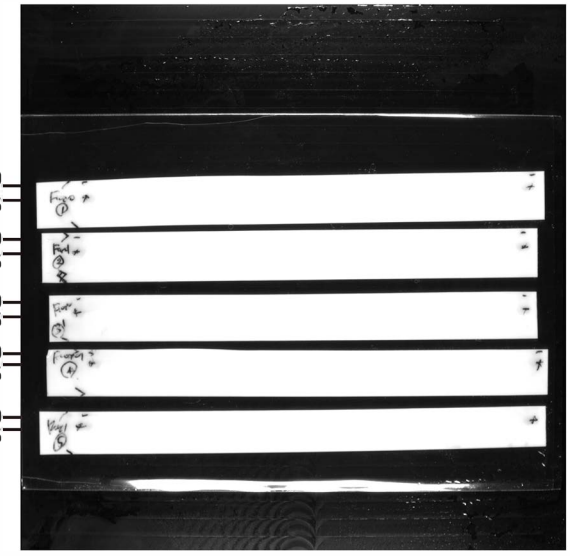

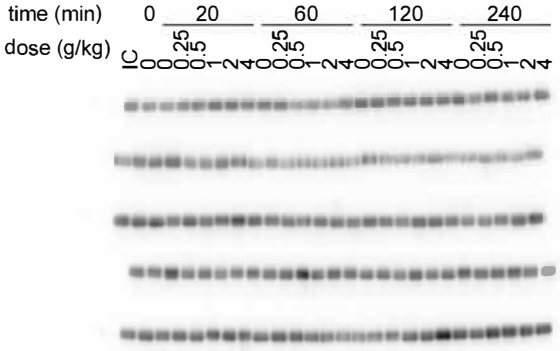

total Irb

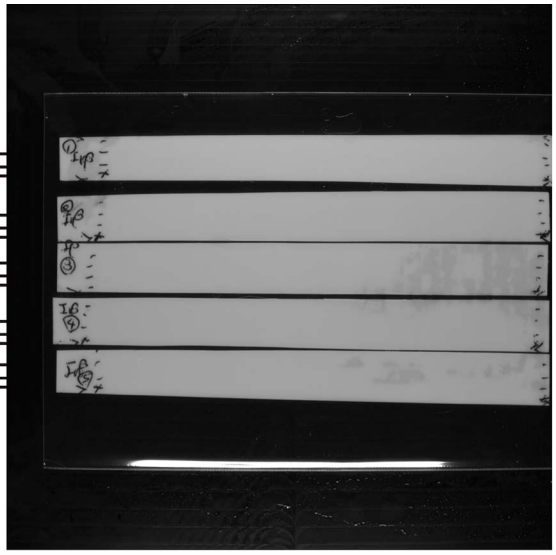

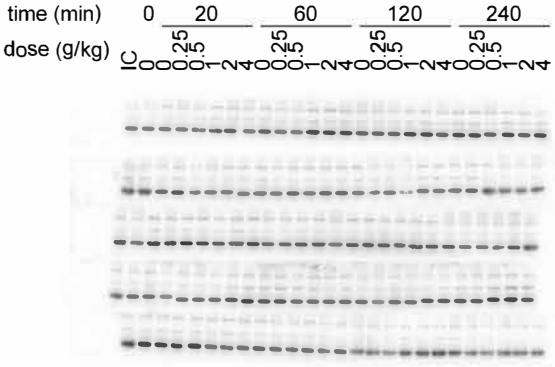

total-Irs1

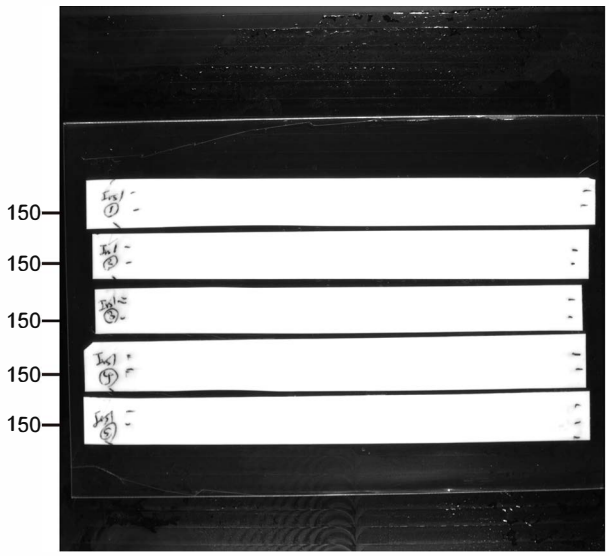

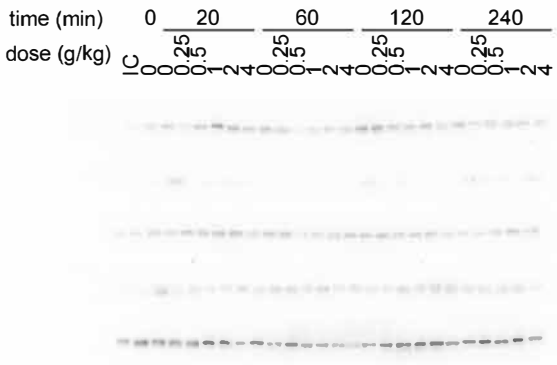

total-Irs2

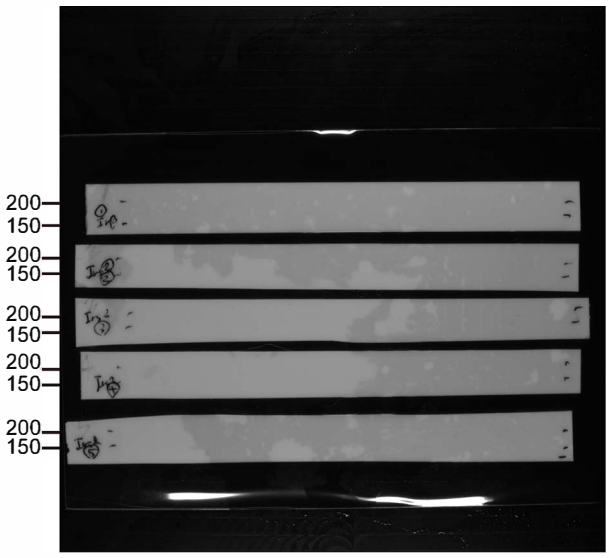

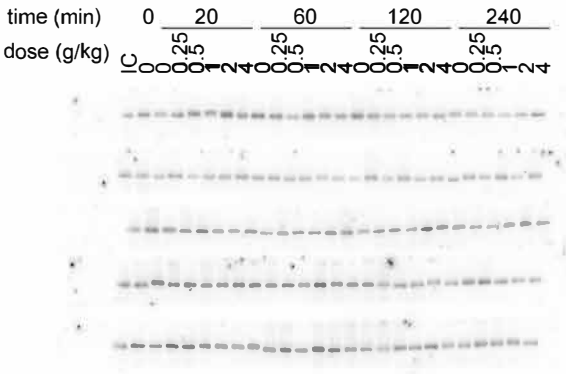

total-mTor

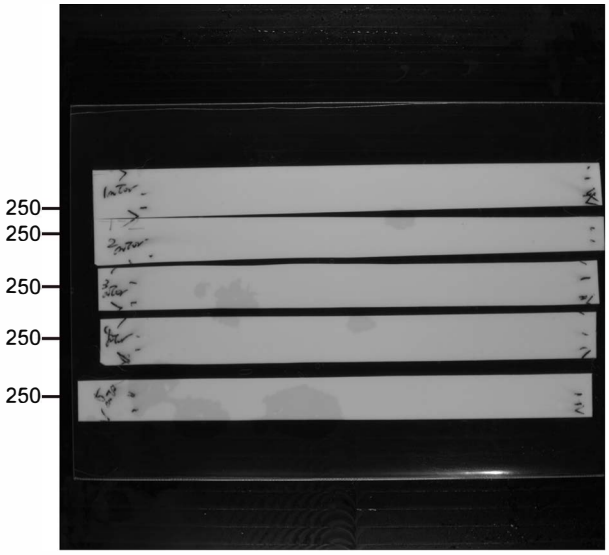

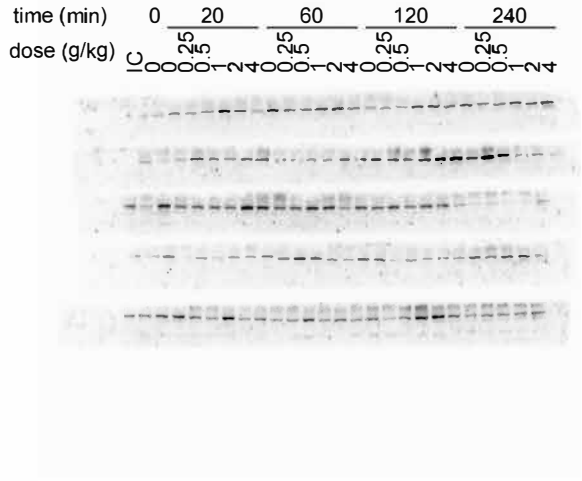

total-S6

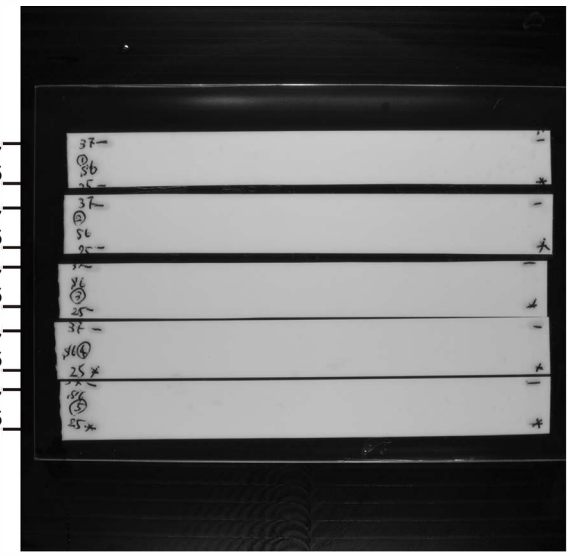

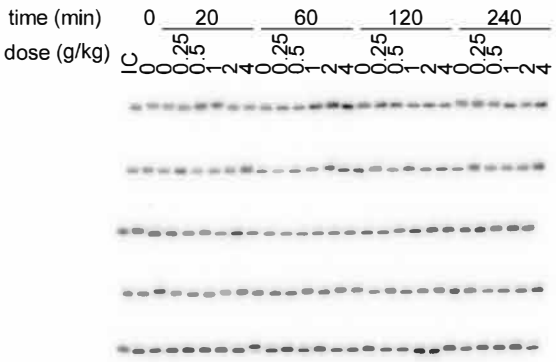

total S6k

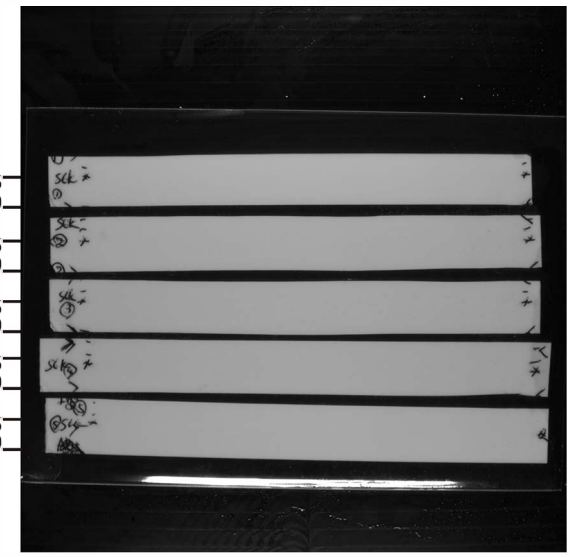

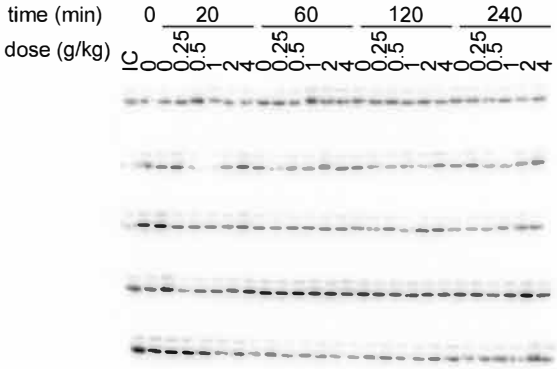

total-Eif4e

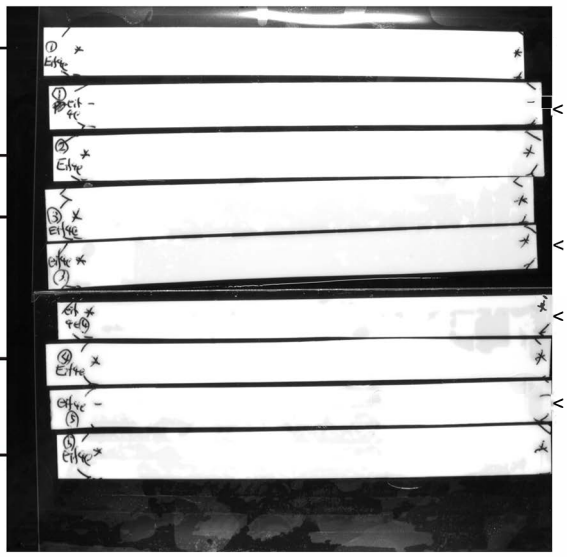

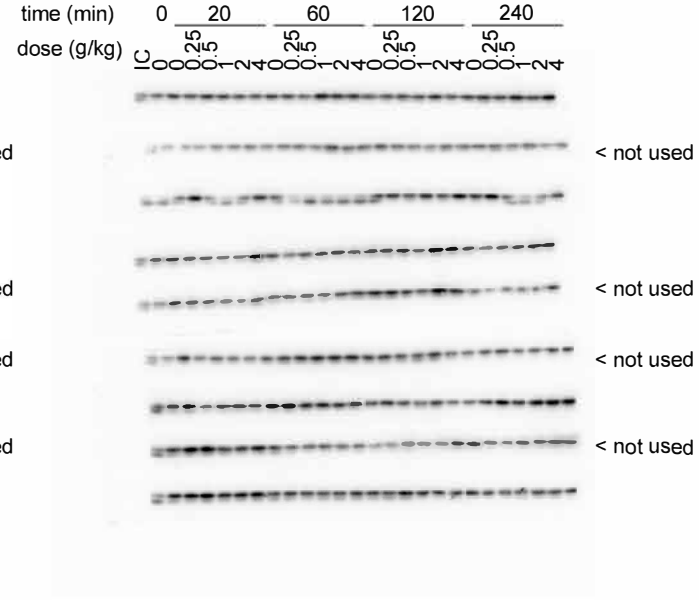

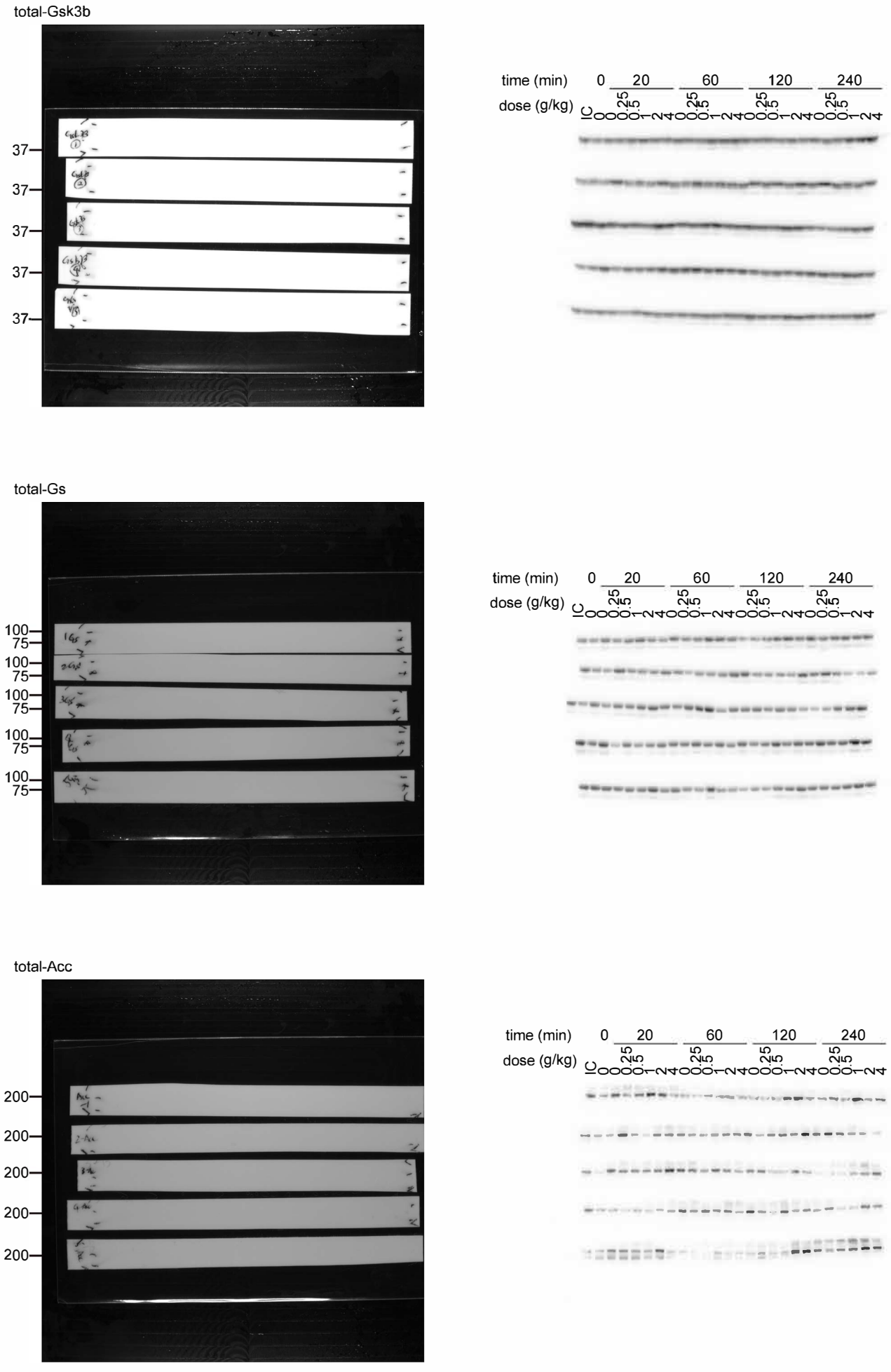

Supplementary Figure 14, Uncropped and unprocessed scans after exporting from the Fusion System Solo 7S of the images displayed in Supplementary Figure 6. Left images are for size markers and right images are for the Chemi-Lumi signals. Note that the order of the membranes was inversed to that of in Supplementary Figure 6 for phospho-Irb. Some membranes those were not used in the following analyses were included to avoid cropping and denoted as "not used".